Controlled rotation of birefringent particles in an optical trap

Kurt D. Wulff,[1,*] Daniel G. Cole,[2] and Robert L. Clark[1,3]

[1]Center for Biologically Inspired Materials and Material Systems, Duke University, Durham, North Carolina 27708, USA

[2]Department of Mechanical Engineering and Materials Science, University of Pittsburgh, Pittsburgh, Pennsylvania 15261, USA

[3]Professor and Dean School of Engineering and Applied Sciences, University of Rochester, Rochester, New York 14620, USA

*Corresponding author: kurt.wulff@duke.edu

Received 31 March 2008; revised 24 October 2008; accepted 25 October 2008; posted 28 October 2008 (Doc. ID 94238); published 26 November 2008

Optical traps have been used in a multitude of applications requiring the sensing and application of forces. However, optical traps also have the ability to accurately apply and sense torques. Birefringent particles experience a torque when trapped in elliptically polarized light. By measuring the frequency content of the exiting beam, the rotational rates can be set up in a feedback loop and actively controlled. Here we describe an optical trap with feedback torque control to maintain constant rotational rates despite the introduction of an increased drag on the particle. As a result, this research has the potential to advance the understanding of rotary motor proteins such as F1 ATPase. © 2008 Optical Society of America

OCIS codes: 120.4640, 140.7010, 350.4855.

1. Introduction

Optical traps have become an important tool in the physical and biological sciences because of their ability to manipulate microscopic particles. The various forms of optical traps, single-beam, two-beam, and levitating, have been used to manipulate objects such as neutral particles [1], viruses and bacteria [2], cells [3], chromosomes and DNA [4–9], and biological motors and motor proteins [10–14]. Many of these configurations were constructed with position and force control. For the construction of force transducers, actuators were readily available with acousto-optical deflectors, spatial light modulators, translation stages, and fast steering mirrors, while position sensors such as direct video measurement, quadrant photodiodes, and interferometric techniques were developed later.

The same steps of developing actuators and sensors for force control are being taken to apply torques to trapped particles. Torque can be applied by using light's spin or orbital angular momentum. In 1936, Beth measured the spin angular momentum of circularly polarized light on a quartz wave plate [15]. Recent experiments have used spin [16–18] as well as orbital angular momentum [19,20] to apply torque to trapped particles. Laser beams with well-defined angular momentum, such as Laguerre–Gaussian beams [21,22], and other beams with phase singularities, such as Bessel beams [23], have also been used to rotate particles. All of these examples are methods that can serve as actuators. The methods used to sense rotational rates varies. Asymmetries have been introduced to allow for the determination of the power spectrum of rotating particles [24]. The direct measurement of the torque transfer to trapped particles has been tracked as well [18,25–27]. Video methods have also been used [28].

By combining actuation and sensing, one is able to control both the angular displacements of and torques applied to trapped particles. This was first accomplished by La Porta and Wang in 2004 [26]. Here,

0003-6935/08/346428-06$15.00/0

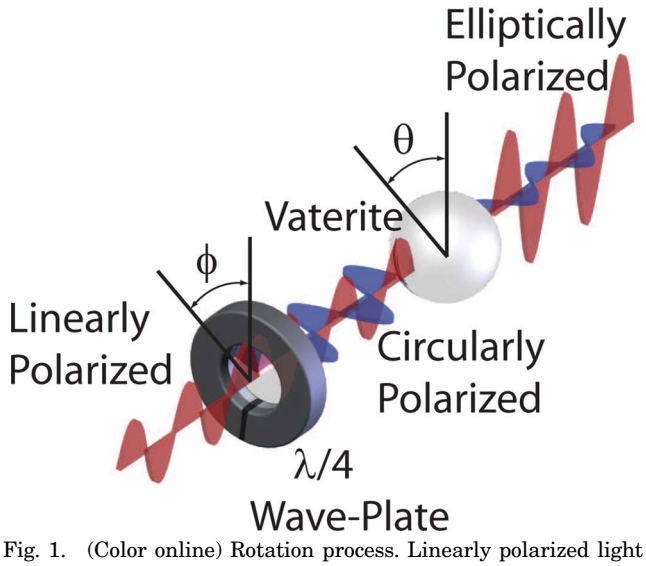

Fig. 1. (Color online) Rotation process. Linearly polarized light enters a quarter-wave plate, is converted to circularly polarized light, and then passes through a birefringent particle (vaterite). Angular moment is transferred to the particle, causing it to rotate. The resulting light exiting the particle is elliptically polarized.

a method is presented to control torque applied to birefringent particles rotating in elliptically polarized light (see Fig. 1). The polarization of the light is modulated to apply torque, and a simple sensor is used to quantify the error from a prescribed angular frequency. With this combination one is able to maintain a constant angular frequency, even in the presence of an increasing load.

2. Theory

Optical traps are possible because each photon of light possesses momentum. The linear momentum flux per photon is $p = \hbar\omega/c$, where $\hbar$ is Planck's constant, ω is the angular frequency of the light, and c is the speed of light. The total momentum flux of a laser beam with power P is $p_z = P/c$. Torques are applied by using light's angular momentum. For circularly polarized Gaussian beams, each photon has an angular momentum of $\pm\hbar$ about the beam axis, equivalent to an angular momentum flux of $\pm P/\omega$ [15]. An elliptically polarized beam has a resulting angular momentum flux of $L_z = \sigma_z P/\omega$, where $\sigma_z = 0, \pm 1$ for linearly and circularly polarized light, respectively, and fractional values for elliptically polarized light [29]. A quarter-wave plate can convert linearly polarized light into elliptically and circularly polarized light, depending on the angle the wave plate makes with respect to the electric field vector.

While partially absorbing particles have been shown to rotate in circularly polarized light [30], faster rotation rates are possible by using birefringent materials. Birefringent materials have a crystalline structure that leads to an anisotropic refractive index. This results in two different orthogonal indices of refraction and a polarization dependent phase delay of

$$\Gamma = k_r d(n_o - n_e). \tag{1}$$

The phase delay is dependent on the wavelength of the light (wavenumber, k_r), the ordinary and extraordinary indices of refraction, n_o and n_e, and the thickness of the birefringent particle, d.

A laser beam passing through a birefringent material of constant thickness experiences a torque due to the spin angular momentum according to

$$\tau = -\frac{\epsilon}{2\omega}E_0^2 \sin\Gamma \cos 2\phi \sin 2\theta + \frac{\epsilon}{2\omega}E_0^2\{1 - \cos\Gamma\}\sin 2\phi, \tag{2}$$

where ϵ is the permittivity, E_0 is the electric field amplitude, ϕ is the ellipticity of the light, and θ is the angle between the fast axis of the quarter-wave plate and the optic axis of the birefringent particle [16,31]. This equation is valid only for birefringent particles of uniform thickness. While not exact for other shapes, or for the nonparaxial beam associated with optical traps, the solution can be used as an estimate of the torque applied to the particles and a physical explanation of how the system works. The first term of Eq. (2) gives the torque applied to a particle by the linearly polarized portion of the light; the second term is the torque due to the circularly polarized portion of the light. The particle will undergo a rotation only when the circularly polarized portion is larger than the linearly polarized portion. The maximum rotational rates will occur when the incoming laser is circularly polarized, that is, $\phi = \pi/4$. This rotational rate can be increased further by increasing the power of the laser beam.

The resulting rotational frequencies and angular displacements can be determined by solving the equation of motion. We will designate two constants to simplify the notation:

$$C_1 = \frac{\epsilon E_0^2}{2\omega}\sin\Gamma\cos 2\phi, \tag{3}$$

$$C_2 = \frac{\epsilon E_0^2}{2\omega}\{1 - \cos\Gamma\}\sin 2\phi. \tag{4}$$

This results in an equation of motion for the rotational system according to

$$I\ddot{\theta} + \beta\dot{\theta} = -C_1 \sin 2\theta + C_2, \tag{5}$$

where I is the mass moment of inertia and β is the rotational Stoke's drag coefficient (for a sphere, $\beta = 8\pi\mu r^3$). Owing to the dominance of viscous forces in the fluid medium, the inertial effects can be considered negligible to simplify the equation to

$$\beta\dot{\theta} = -C_1 \sin 2\theta + C_2. \tag{6}$$

By making a change of variable, $y = 2\theta$ and $\dot{y} = 2\dot{\theta}$, and setting $a = 2C_2/\beta$, $b = -2C_1/\beta$, we end up with the resultant integral equation

$$\int \frac{\mathrm{d}y}{a + b \times \sin y} = t + C$$
$$= \frac{2}{\sqrt{a^2 - b^2}} \tan^{-1}\left(\frac{a \tan\frac{y}{2} + b}{\sqrt{a^2 - b^2}}\right), \quad (7)$$

where t represents time. We can assume that $|a| \gg |b|$, since C_2 will be the larger component when particles are rotating. Also, we can assume that at large times, t, C' is small, so this simplifies the equation to

$$y \simeq \sqrt{a^2 - b^2}\, t. \quad (8)$$

This can be expressed in terms of θ:

$$\theta = \frac{\sqrt{C_2^2 - C_1^2}}{\beta} t. \quad (9)$$

Taking the time derivative of Eq. (8) yields $\dot{\theta}$:

$$\dot{\theta} = \frac{\sqrt{C_2^2 - C_1^2}}{\beta}$$
$$= \frac{P}{\omega\beta}(\{1 - \cos\Gamma\}^2 \sin^2 2\phi - \sin^2\Gamma \cos^2 2\phi)^{1/2}. \quad (10)$$

It is important to realize that this result is the average rotational speed of a trapped particle, since we are assuming large times. This is obvious from Eq. (2), since the torque, τ, fluctuates as a function of the axis of the birefringent particle when the light is not circularly polarized. Also, the particle will rotate only when C_2 is greater than C_1. This physically relates to the particle's crystalline axis aligning with the linearly polarized portion of the laser. If ϕ is too small, the alignment torque inhibits rotation.

3. Experimental Methods

The optical trap is built with an inverted microscope, a Nd:YAG laser ($\lambda = 1064$ nm), and a high numerical aperture objective (Zeiss Plan-Apochromat $63\times$/1.4 NA; see Fig. 2). The objective is designed for Nomarski DIC microscopy, which is important in this application, since it preserves the polarization of the incoming beam.

The polarization of the trapping laser is modulated by controlling the angle of a quarter-wave plate. The wave plate is mounted in a custom-built rotational stage positioned in front of the epifluorescence port (see Fig. 2). It is necessary to place this as close to the objective as physically possible in order to preserve the polarization of the light. The rotational stage consists of a wave plate mounted in a bearing that is driven by a stepper motor. A potentiometer is incorporated in the gear train to sense the angular position of the wave plate. The angle of the wave plate is maintained through closed-loop control.

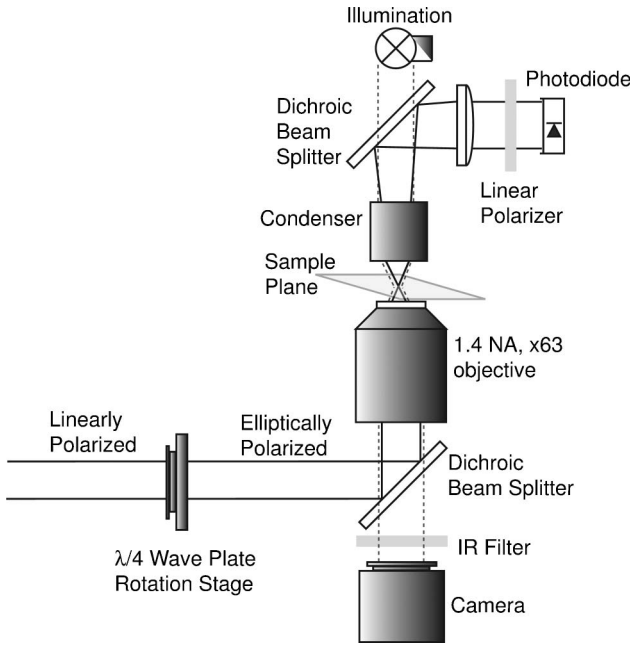

Fig. 2. Schematic of the optical trapping setup for rotating birefringent particles. The linearly polarized laser beam is converted to elliptically polarized light through a quarter-wave plate mounted in a rotational stage, which rotates trapped birefringent particles. The forward scattered laser is projected onto a quadrant photodiode to track the rotational frequency of the particle.

After the laser passes through the sample, the forward scattered light is collected by a high-NA condenser (Zeiss Achromatic-aplanatic condenser 1.4 NA). The laser beam is separated from the illumination by a dichroic mirror located above the condenser. The dichroic mirror directs the laser through a polarizing beam splitting cube and onto a quadrant photodiode. The intensity signal is antialias filtered and digitized by using a dSPACE data acquisition board.

The rotational speed of the trapped particle is measured by analyzing the intensity of the laser signal on the quadrant photodiode (see Fig. 3). While it is possible to measure the rotational frequency directly by taking an autospectrum of the intensity signal, this approach was not chosen because of the computational constraints of block processing and the need to have the faster sensor signal necessary for feedback control. Instead, a method that is usable in a feedback control scheme was developed. The intensity fluctuations are first detrended by using a high-pass filter to remove the DC component of the signal. The signal is then split onto two paths for simultaneous high- and low-pass filtering with each filter having the same cutoff frequency. The cutoff frequency is selected to be in the middle of the range of desired rotational frequencies. The RMS value of each signal is then computed and integrated to give the relative sizes. The signals are then subtracted from each other. The result is not the

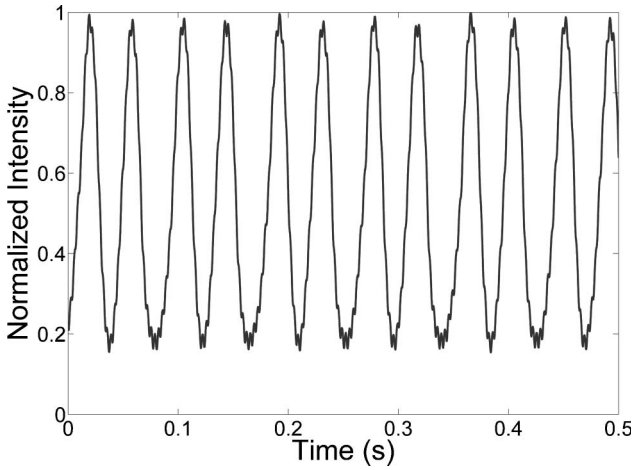

Fig. 3. Intensity fluctuations of a rotating particle. The particles do not rotate perfectly about the axis of the laser. This produces a sinusoidal response signal at the frequency of rotation, which can be traced in the measured intensity of the forward scattered laser. This intensity fluctuation is critical to the rotational tracking. This particle is rotating at ~24 Hz.

rotational frequency but rather an error from which the actual rotational frequency can be calculated. This method is essentially a frequency comparing system to give an error signal. A block diagram representation of this is illustrated in Fig. 4.

The actual rotational frequency can be calculated from the error signal. To do this, the error sensor was first simulated by using a swept sine input, the results of which are presented in Fig. 5. Because both the error and the corresponding input are known, these data could then be used in a lookup table to convert error signals into actual frequencies. This lookup table would be independent of size, since it is based on the fluctuations of the intensity signals. The results were computed with the cutoff frequencies of the high- and low-pass filters set to 25 Hz. This value was chosen to give the most dynamic range between the frequencies of 10 and 50 Hz.

A limitation to this method is that the particles must be rotating above 10 Hz for an accurate measurement. This is not an issue if the particle is already rotating, since most particles rotate faster than 10 Hz. The frequency sensor is also limited in the speed of its response. The sensor is an averaging sensor of the rotational frequencies, and therefore the speed of this sensor is limited by the low-pass filter used in the RMS process. Even though the sensor is limited, the response times are still much greater than performing an autospectrum to gain frequency content, which is the reason that this method was chosen. Also, the sensing system can measure only the magnitude of the rotational frequency; the direction remains unknown in this method.

4. Experimental Results

The goal of this research is to build a method to regulate the rotational rates of birefringent microscopic particles. As stated in Section 2, this can be accomplished by modulating either the polarization or the power of the trapping laser. In these experiments only the polarization will be controlled, since actively controlling the power was seen as potentially harmful to the trapping laser. This also allows the ability to maintain a trapped particle and servo control the angular displacement.

The experiments were carried out by using the birefringent material vaterite. Vaterite is an easily produced, positive uniaxial, birefringent material with $n_o = 1.55$ and $n_e = 1.65$ [25]. Vaterite also forms as a spherical particle, making the viscous drag easier to calculate. Using a purely circularly polarized beam, vaterite particles have been rotated at rates of 400 Hz. To determine the effect of the angle of the quarter-wave plate, ϕ, on the rotational rates, a vaterite particle ($d \sim 4\,\mu$m) was trapped while the angle of the wave plate was incrementally moved 90°. At each angle, an autospectrum was calculated to determine the rotational frequency. The results for these particles were consistently ~10–60 Hz with

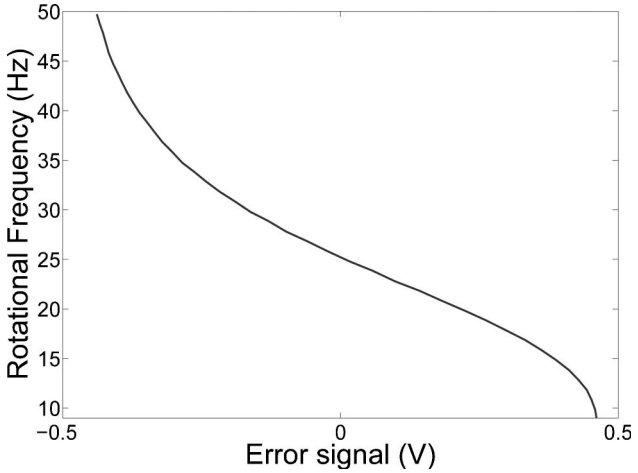

Fig. 5. Error signal versus input frequency for a simulated response of the rotational error sensor. The cutoff frequencies of the low- and high-pass filters were both set at 25 Hz.

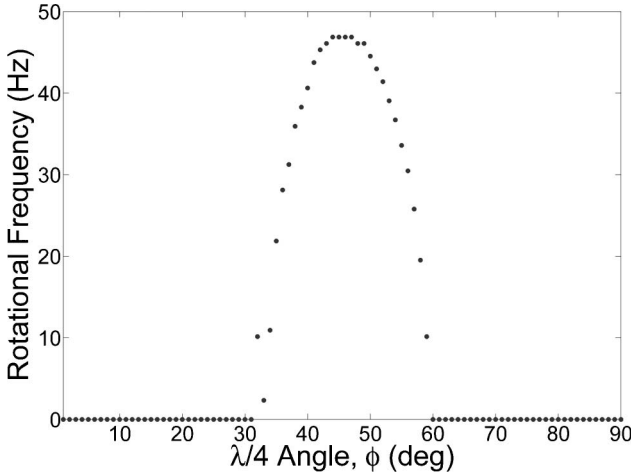

Fig. 6. Experimental results of the rotational frequency of a 4 μm vaterite particle versus the angle (ϕ) of the quarter-wave plate.

the maximum rotational frequency when the light was circularly polarized ($\phi = 45°$; see Fig. 6). The direction of the rotation can be switched by rotating the wave plate from −90° to 0°, which effectively switches the handedness of the polarization. Through analysis of Fig. 6, it is important to note that the rotational frequencies are not a linear function of the angular position. Also, rotation occurs only over a 27° window, and half of that window is a duplicate of the first half. This translates to a 13.5° range for rotational control.

Using these results, an open-loop controller can be constructed. However, if the particle experiences a variable load due to viscous drag (e.g., bringing the sample closer to the surface), or if the particle is tethered, for example, to a rotatory motor protein, the rotational frequencies will not remain constant. As a result, a closed-loop servo controller was implemented. Many controller design techniques were not available because of the complex characteristics of the system. Owing to these complexities as well as those of the system associated with the stepper motor dynamics, the PI (proportional-integral) controller was tuned by Ziegler–Nichols tuning methods. A block diagram of the controller is presented in Fig. 7.

The servo control of rotational frequencies is accomplished by entering a reference frequency. The reference signal is then compared with the actual signal to generate an error. The error signal is altered by the controller, K, which produces a command angle, ϕ, that directs the angular position of the wave plate. The angle of the wave plate is constrained to be $0 \le \phi \le 45$, since angles greater than 45° reduce the rotational frequency, and would, in effect, switch the sign of the controller.

A PI controller was implemented, and its performance was verified by observing the system's response to a step input. Because of the limitations of the sensor, the particle had to be rotating initially. Since 25 Hz is the cutoff frequency of the sensor, a step input from that to 30 Hz was used (see Fig. 8). The system has a rise time of 0.77 s and settles within 1 Hz of the desired frequency.

Taking into account the system's limitations, these results are expected. The response of the controller is primarily limited by the sensor, which is an averaging process with a time characteristic of one cycle. Each cycle is ~1 Hz, so a response much faster than 1 Hz is not possible. A faster sensing method is needed to further push this limit. Even in the presence of a faster responding sensor, the particle's rotational speed is not constant, as it fluctuates at twice the rotational velocity. This is due to the constant acceleration of the particle to align its birefringent axis with the linearly polarized portion of the light. This is also a limitation of the system.

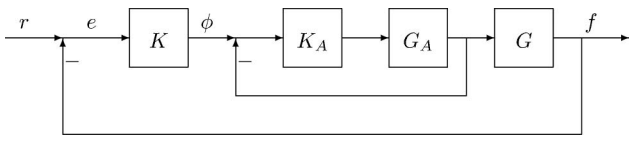

Fig. 7. Block diagram representation of the rotational control system with feedback control. The rotating particle as well as the sensor dynamics are represented as G, while K represents the controller. G_A and K_A represent the rotational stage and its controller.

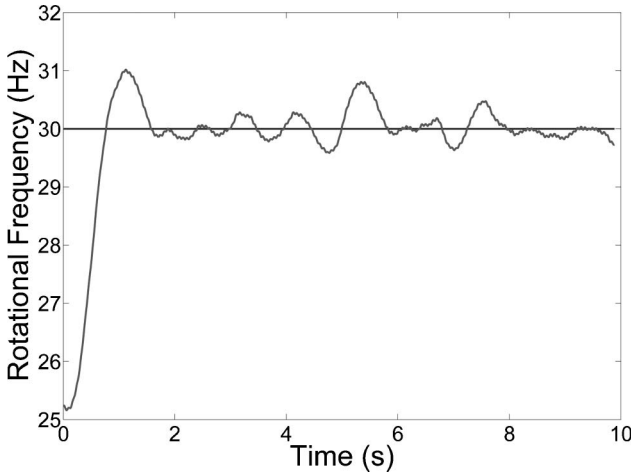

Fig. 8. Step response of a 4 μm vaterite particle from 25 to 30 Hz. The rise time is 0.77 s, and the controller stabilizes the system to within 1 Hz of the desired frequency.

5. Conclusions

A rotational feedback control system was successfully implemented and demonstrated by modulating the polarization of the trapping laser. The polarization was controlled through the use of a quarter-wave plate mounted in a rotational stage. The rotational sensor was capable of sensing the error from a specific frequency, which was then converted to a measured frequency. The sensor, however, severely limits the speed of response of the system. The bandwidth of the sensor is ultimately defined by the bandwidth of the integrating filter in the system used to calculate the RMS response of the high- and low-passed signals. This frequency was of the order of 1 Hz.

The measured frequencies are also an averaged frequency of the particle. This is due to the optic axis of the birefringent particle aligning with the linearly polarized component of the incoming electric field. Also, depending on the size of the particle, the effective polarization window for angular control changes. Typically, particles of the order of 4 μm would rotate between the angles of 30° and 45°, while smaller particles tended to have smaller angular windows. Each particle size required an individual controller to be designed for them, since each particle's rotation window and viscous drag was different. Self-tuning or adaptive controllers could be used to tune controllers for different sized particles.

The selection of the rotational frequency also was crucial. It was important to select a frequency within 5 Hz of the maximum rotational frequency but not outside the capabilities of the particle. This results in a nearly linear error sensor around the center

frequency. Failure to do so did not give the controller adequate range for control.

The work performed here successfully applied control to rotational particles by manipulating the polarization of the trapping beam. This work has the potential to be used to apply torque to biological samples tethered to a birefringent particle, or for use as a highly sensitive micropump.

This work was generously supported by National Science Foundation (NSF) Integrative Graduate Research Traineeship (IGERT) grant DGE-0221632.

References

1. A. Ashkin, *Optical Trapping and Manipulation of Neutral Particles Using Lasers* (World Scientific, 2006).
2. A. Ashkin and J. M. Dziedzic, "Optical trapping and manipulation of viruses and bacteria," Science **235**, 1517–1520 (1987).
3. A. Ashkin, J. M. Dziedzic, and T. Yamane, "Optical trapping and manipulation of single cells using infrared laser beams," Nature **330**, 769–771 (1987).
4. M. W. Berns, W. H. Wright, B. J. Tromberg, G. A. Profeta, J. J. Andrews, and R. J. Walter, "Use of a laser-induced optical force trap to study chromosome movement on the mitotic spindle," Proc. Natl. Acad. Sci. USA **86**, 4539–4543 (1989).
5. S. Chu, "Laser manipulation of atoms and particles," Science **253**, 861–866 (1991).
6. T. T. Perkins, D. E. Smith, and S. Chu, "Direct observation of tube-like motion of a single polymer-chain," Science **264**, 819–822 (1994).
7. S. B. Smith, Y. J. Cui, and C. Bustamante, "Overstretching B-DNA: the elastic response of individual double-stranded and single-stranded DNA molecules," Science **271**, 795–799 (1996).
8. M. D. Wang, H. Yin, R. Landick, J. Gelles, and S. M. Block, "Stretching DNA with optical tweezers," Biophys. J. **72**, 1335–1346 (1997).
9. G. J. L. Wuite, R. J. Davenport, A. Rappaport, and C. Bustamante, "An integrated laser trap/flow control video microscope for the study of single biomolecules," Biophys. J. **79**, 1155–1167 (2000).
10. A. D. Mehta, M. Rief, J. A. Spudich, D. A. Smith, and R. M. Simmons, "Single-molecule biomechanics with optical methods," Science **283**, 1689–1695 (1999).
11. T. Strick, J. F. O. Allemand, V. Croquette, and D. Bensimon, "The manipulation of single biomolecules," Phys. Today **54** (10), 46–51 (2001).
12. J. E. Molloy, J. E. Burns, J. Kendrickjones, R. T. Tregear, and D. C. S. White, "Movement and force produced by a single myosin head," Nature **378**, 209–212 (1995).
13. C. Veigel, J. E. Molloy, S. Schmitz, and J. Kendrick-Jones, "Load-dependent kinetics of force production by smooth muscle myosin measured with optical tweezers," Nat. Cell Biol. **5**, 980–986 (2003).
14. K. Visscher, M. J. Schnitzer, and S. M. Block, "Single kinesin molecules studied with a molecular force clamp," Nature **400**, 184–189 (1999).
15. R. A. Beth, "Mechanical detection and measurement of the angular momentum of light," Phys. Rev. **50**, 115–127 (1936).
16. M. E. J. Friese, T. A. Nieminen, N. R. Heckenberg, and H. Rubinsztein-Dunlop, "Optical alignment and spinning of laser-trapped microscopic particles," Nature **394**, 348–350 (1998).
17. M. E. J. Friese, H. Rubinsztein-Dunlop, J. Gold, P. Hagberg, and D. Hanstorp, "Optically driven micromachine elements," Appl. Phys. Lett. **78**, 547–549 (2001).
18. A. I. Bishop, T. A. Nieminen, N. R. Heckenberg, and H. Rubinsztein-Dunlop, "Optical application and measurement of torque on microparticles of isotropic nonabsorbing material," Phys. Rev. A **68**, 033802 (2003).
19. N. B. Simpson, K. Dholakia, L. Allen, and M. J. Padgett, "Mechanical equivalence of spin and orbital angular momentum of light: an optical spanner," Opt. Lett. **22**, 52–54 (1997).
20. H. He, M. E. J. Friese, N. R. Heckenberg, and H. Rubinsztein-dunlop, "Direct observation of transfer of angular-momentum to absorptive particles from a laser-beam with a phase singularity," Phys. Rev. Lett. **75**, 826–829 (1995).
21. L. Allen, M. W. Beijersbergen, R. J. C. Spreeuw, and J. P. Woerdman, "Orbital angular-momentum of light and the transformation of Laguerre–Gaussian laser modes," Phys. Rev. A **45**, 8185–8189 (1992).
22. S. M. Barnett and L. Allen, "Orbital angular-momentum and nonparaxial light-beams," Opt. Commun. **110**, 670–678 (1994).
23. V. Garcés-Chávez, K. Volke-Sepulveda, S. Chávez-Cerda, W. Sibbett, and K. Dholakia, "Transfer of orbital angular momentum to an optically trapped low-index particle," Phys. Rev. A **66**, 063402 (2002).
24. A. D. Rowe, M. C. Leake, H. Morgan, and R. M. Berry, "Rapid rotation of micron and submicron dielectric particles measured using optical tweezers," J. Mod. Opt. **50**, 1539–1554 (2003).
25. A. I. Bishop, T. A. Nieminen, N. R. Heckenberg, and H. Rubinsztein-Dunlop, "Optical microrheology using rotating laser-trapped particles," Phys. Rev. Lett. **92**, 198104 (2004).
26. A. La Porta and M. D. Wang, "Optical torque wrench: Angular trapping, rotation, and torque detection of quartz microparticles," Phys. Rev. Lett. **92**, 190801 (2004).
27. T. A. Nieminen, N. R. Heckenberg, and H. Rubinsztein-Dunlop, "Optical measurement of microscopic torques," J. Mod. Opt. **48**, 405–413 (2001).
28. E. Higurashi, H. Ukita, H. Tanaka, and O. Ohguchi, "Optically induced rotation of anisotropic micro-objects fabricated by surface micromachining," Appl. Phys. Lett. **64**, 2209–2210 (1994).
29. T. A. Nieminen, H. Rubinsztein-Dunlop, N. R. Heckenberg, and A. I. Bishop, "Numerical modelling of optical trapping," Comput. Phys. Commun. **142**, 468–471 (2001).
30. M. E. J. Friese, T. A. Nieminen, N. R. Heckenberg, and H. Rubinsztein-Dunlop, "Optical torque controlled by elliptical polarization," Opt. Lett. **23**, 1–3 (1998).
31. K. C. Neuman and S. M. Block, "Optical trapping," Rev. Sci. Instrum. **75**, 2787–2809 (2004).